

# THE DEFORMATION OF ALKALI-ACTIVATED MATERIALS AT DIFFERENT CURING TEMPERATURES

MARK ČEŠNOVAR<sup>1,2</sup>, KATJA TRAVEN<sup>1</sup> & VILMA DUCMAN<sup>1</sup>

<sup>1</sup> Slovenian National Building and Civil Engineering Institute (ZAG), Ljubljana Slovenia, e-mail: mark.cesnovar@zag.si, katja.traven@zag.si, vilma.ducman@zag.si

<sup>2</sup> International Postgraduate School Jozef Stefan, Ljubljana, Slovenia, e-mail: mark.cesnovar@zag.si

**Abstract** Alkali activation is a chemical process whereby materials rich in aluminosilicate, which dissolves in basic media at room temperature, form binding phases by polycondensation. The alkali-activated materials (AAM) are a promising alternative to binding materials such as cement or other products in civil engineering (van Deventer et al., 2012). This study investigates the early age shrinkage behavior of Slovenian ladle and electric arc furnace slag-based alkali activated materials at different curing temperatures. The dimensions of specimens cured at room temperature and elevated temperatures up to 90 °C were measured over the first 7 hours (every 10 min). The results show that the most shrinkage occurred at the highest temperature, owing to the highest rate of evaporation of liquid content. Loss of mass follows from the drying shrinkage.

## Keywords:

alkali-activated materials, ladle slag, electric arc furnace slag, shrinkage, cracks.

## 1 Introduction

Alkali-activated materials (AAM) have been widely studied in recent years because of a desire to produce more sustainable materials with less environmental impact. The high potential of AAM results from the availability of raw materials such as metallurgical slag, fly ash etc., which often accumulate in landfills as industrial by-products (Natali Murri *et al.*, 2013). Given that alkali activation is a low energy technology, these materials could offer an economic and environmentally friendly alternative to ordinary building materials (Fernandez-Jimenez *et al.*, 2015). Although AAM could be useful as a concrete binder, brick or lightweight insulation material, the composition of the raw material and the processing parameters can strongly affect the physical properties. Most of the factors that influence the micro-structural evaluation and/ or mechanical properties of AAM have, however, already been studied, including raw materials (chemical properties) (Fernandez-Jimenez *et al.*, 2006), Al/Si (composition) ratios (van Jaarsveld *et al.*, 2002), activator (Chen *et al.*, 2017), curing regime and ageing (Češnovar *et al.*, 2019). Shrinkage has been widely studied in the ordinary Portland cement system and is also relevant for AAM. For OPC concrete, it is well known that four types of shrinkage occur: plastic, drying, autogenous and carbonation shrinkage. Plastic shrinkage is an immediate after-effect of casting, when water evaporates. Drying shrinkage is the result of dehydration from the gel pores, and autogenous shrinkage is caused by self-desiccation that is a result of higher capillary forces when smaller pores are formed. Carbonation deformation is the result of the penetration of CO<sub>2</sub> from air into concrete, and it has not yet been confirmed in the AAM system. Some studies reported expansion of AAM at certain curing stages, where samples were cured under controlled humidity conditions, so such expansion cannot be the result of autogenous deformation, according to the desiccation theory for OPC (Mobili *et al.*, 2016). Chemical shrinkage or expansion is where the absolute volume change of material occurs as a result of chemical reactions (Lura *et al.*, 2003). The correlation between the deformation and reaction processes was extensively studied by Li *et al.* with a metakaolin geopolymer system, where three stages of chemical shrinkage occur. Within the first few hours, the dissolution of aluminosilicates causes shrinkage; after approximately 8 hours, the formation of Al- rich products consisting of gels (nano-zeolites) takes place along with expansion and is followed by shrinkage when the Al species are further polymerized with available silicate oligomers to produce an Si-rich network (Li *et al.*, 2019). Deformation associated with the curing of AA pastes at room temperature or

when exposed to a slightly elevated temperature has a strong impact on the mechanical properties of materials (Mastali *et al.*, 2018, Gudmundsson *et al.*, 2013). Different curing temperatures cause autogenous, chemical and drying shrinkage, with cracking and microstructure deformation, especially during alkali activation and in the early stage of curing when chemical reactions and autogenous shrinkage take place. Current studies show that autogenous shrinkage could be more problematic than drying shrinkage because it develops quickly at the time when the strain on the material is low (Nedeljković *et al.*, 2018, Jensen *et al.*, 2001). The overall deformation in AAM is mostly a result of chemical reactions and water evaporation (drying) from the AA pastes. During the AA process, as incorporated water evaporates from the paste at room temperature and with low humidity, the volume of AA bodies reduces, and cracking occurs owing to capillary pressure between wet and dry micropore areas (Mastali *et al.*, 2018, Li *et al.*, 2018).

The goal of the present study was to assess shrinkage and/or expansion during alkali activation of ladle and electric arc furnace slag, and to further investigate the effect of the curing regime (temperature, time) on shrinkage and mass reduction in order to identify possible causes of deformation.

## 2 Materials and methods

This experimental study used electric arc furnace and ladle slag (hereafter designated Slag A and Slag R) as precursors for alkali activation with potassium water glass ( $K_2SiO_3$ , Betol K5020T, Woellner, Germany). Both slags are from Slovenian metallurgical industries. The chemical composition of both slags, analyzed using an X-ray fluorescence instrument (XRF-Thermo Scientific ARL Perform X, USA), is shown in Table 1.

**Table 1: Chemical composition of Slag A and Slag R used for preparation of AAM (in wt. %).**

	Na <sub>2</sub> O	MgO	Al <sub>2</sub> O <sub>3</sub>	SiO <sub>2</sub>	K <sub>2</sub> O	CaO	Cr <sub>2</sub> O <sub>3</sub>	MnO	Fe <sub>2</sub> O <sub>3</sub>	LOI	OTH
<b>Slag A</b>	0.13	14.87	8.54	21.05	0.17	20.87	3.76	2.24	11.37	14.15	14.15
<b>Slag R</b>	0.28	23.25	5.20	13.69	0.14	27.85	0.18	0.62	4.64	20.47	20.47

The quantitative determination (Rietveld) of mineral phases made from X-ray diffraction analysis (XRD- Malvern PANalytical Empyrean, NL and UK) confirmed that both slags contained a high percentage of amorphous phase (55 wt.% for A and 35 wt.% for R).

Prior to alkali activation, the slags were milled and sieved to under 63  $\mu\text{m}$ . Powder size distribution was measured using a CILAS 920 (Cilas, Orleans Cedex, France), and the specific surface area was analysed using a Micromeritics ASAP 2020, (Micromeritics, Norcross, GA, USA). The average particle size diameter was 5.94  $\mu\text{m}$ , with a specific surface area of 7.61  $\text{m}^2/\text{g}$  for Slag A and 5.45  $\mu\text{m}$ , with a specific surface area 3.52  $\text{m}^2/\text{g}$  for Slag R.

The A and R slags in a 1/1 mass ratio were activated with 33wt. %  $\text{K}_2\text{SiO}_3$  using an activator/slag ratio of 0.6. Pastes were prepared by homogenization with an electric lab. Mixer, as shown in Figure 1 and cast in 120 x 120 x 250  $\text{mm}^3$  moulds. Mixtures of the same composition were cured under different conditions, one at room temperature and the others at an elevated temperature by heating in a laboratory heat-chamber. After 60 min, all samples were demoulded, except for the one cured at room temperature, which was left in the mould because of its low strain.



**Figure 1: Homogenization of AA pastes.**

The length of specimens was measured using a micrometer (Mitutoyo, Kanagawa, JPN) and mass reduction by weighing specimens with a laboratory balance with a precision of  $10^{-4}$  g (Mettler Toledo, Ohio, USA). The measurements and photographs of specimens were taken every 15 minutes of treatment for the first 400 minutes. Shrinkage was calculated according to equation 1.

$$\Delta l = \frac{l_0 - l}{l_0} * 100(\%) \quad (1)$$

Where  $\Delta l$  is the shrinkage,  $l$  is the length of the specimen measured at a given time period and  $l_0$  is the initial length of the specimen after moulding.

### 3 Results and discussion

The deformation and reduction of mass in AAM for the first 7 hours of curing is presented in Figure 2. Plastic shrinkage occurs immediately after casting the AA paste into a mould and continues for 90 minutes, causing low mass reduction in specimens cured at room temperature. A very low percentage of water evaporated from the surface of the specimen at room temperature and the shrinkage could not therefore be detected. The most shrinkage, of 3.5 and 4 %, was detected in the specimens cured at 70 °C and 90 °C after 60 min of curing, and the mass reduction was 2 and 4 % of the original weight, respectively. After shrinkage, expansion takes place after 70 minutes of curing in all specimens, except for the one cured at room temperature. This phenomenon is attributed to chemical expansion, whereby an Al-rich nano-zeolite gel is produced (Li *et al.*, 2019). During this time, the reduction of mass shows that autogenous drying is also present. The expansion due to the chemical process is greater than shrinkage in this time period. For the specimen cured at room temperature, there is no expansion curve in Figure 2a, perhaps because the autogenous shrinkage and chemical expansion compensate for the overall deformation. Moreover, the mass reduction for this specimen presented in the Figure 2b curve at 100 min shows a minimal slope. The difference between curing at room and elevated temperatures could be due to faster water evaporation from the specimens and a higher dynamic of the chemical process where the precursor dissolves in the alkaline media. After approx. 120 min of curing, all the specimens show shrinkage, which is a result of chemical and autogenous or drying shrinkage. The slopes in Figure 2b show the mass reduction for all specimens. As

expected, minimal loss is seen in the specimens cured at room temperature, and mass reduction increases with the elevated temperature.

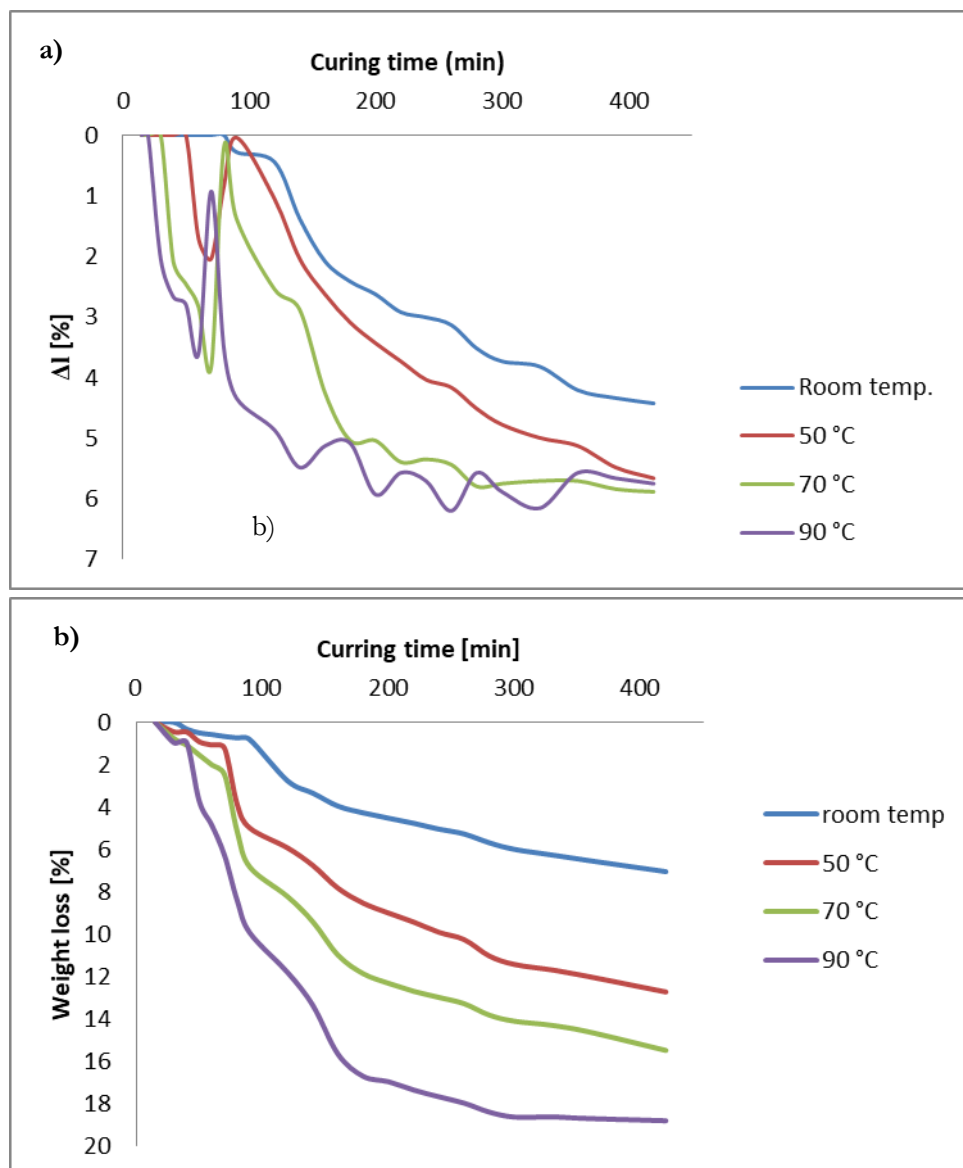
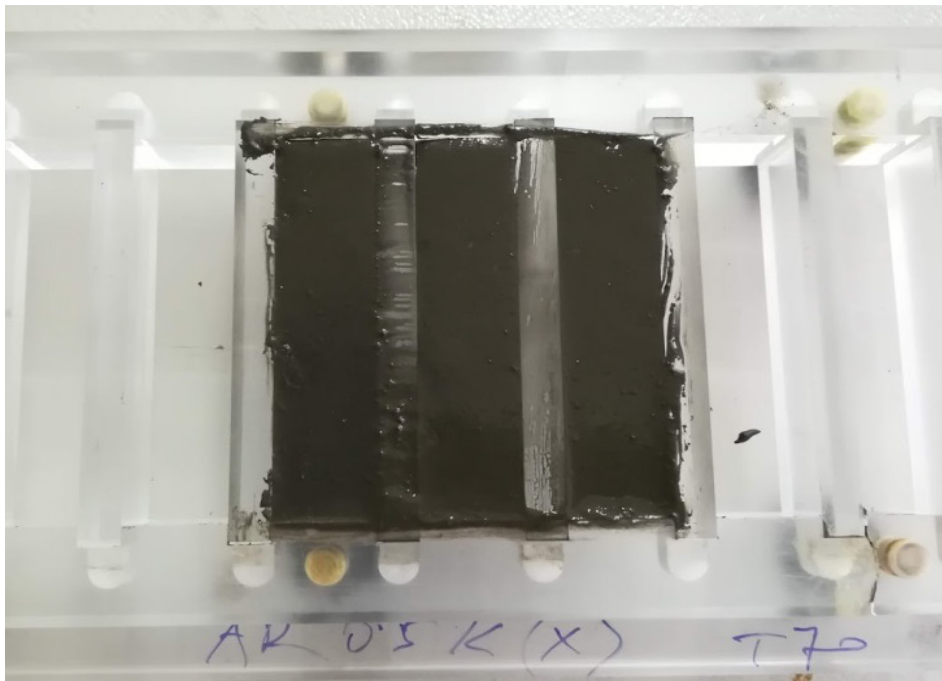














Figure 2: a) Drying shrinkage and b) mass reduction as a function of curing age at room and elevated temperatures.

Specimens were cast in moulds as shown in Figure 3. Pictures of the specimen surfaces studied after various times of exposure and curing at room and at elevated temperature were taken during each measurement and weighing of specimens and are shown in Table 2. They reveal that after the chemical expansion takes place, cracks appear on the surface and inner surface of the specimens and then disappear around the time that expansion with chemical, autogenous and drying shrinkage ends. No specific changes to the surface were observed in specimens cured at room temperature for the first 7 hours. Those cracks that had appeared on the surface of all other specimens after curing for 70 min then totally disappeared at 260 min on the specimen cured at 90 °C and were reduced in size on the specimens cured at lower temperatures. After 300 min of curing, the smaller cracks also disappeared under 50 and 70 °C conditions. Major differences appear with specimens cured at higher temperatures, and that relevance is also shown on the graph in Figure 2b. Specimens treated at room temperature had 4.5 % of shrinkage after 7 hours of curing, while all other specimens resulted in approximately 6 % of shrinkage.



**Figure 3: Samples of AA pastes immediately after casting in the moulds.**

**Table 2: Surface of the specimens as a function of curing time and temperature.**

Curing Time (min) /Temp. (°C)	70	260	300
Room temp.			
50			
70			
90			

As expected, such deformation and cracks significantly influence the mechanical properties. In our previous study of the development of mechanical strength, it was determined that compressive strength varied from 40 to 58 MPa because of the influence of differences in curing temperature (Češnovar *et al.*, 2019), a phenomenon which is now more understandable in the light of the shrinkage/expansion behavior of such materials.



## 4 Conclusions

In this study, dimension and weight measurements were employed to investigate the effect of curing on shrinkage and mass reduction after alkali activation of ladle and electric arc furnace slag. The focus was on the formation of cracks during the drying of specimens. Different curing temperatures were used in order to distinguish among possible causes of deformation, such as plastic, chemical, autogenous and drying expansion or shrinkage of specimens after alkali activation. The mass reduction of specimens cured at room temperature for the first 7 hours showed that the evaporation of water represents the smallest contribution when compared to specimens treated at 90 °C. Nevertheless, specimens treated at room temperature had the least shrinkage, with an absolute value of 4.5 %, compared to 6 % of shrinkage after 7 hours of curing in all other specimens. From the specimens' surface, it is obvious that larger cracks are formed with a higher curing temperature, as confirmed by the deformation slope trend for each specimen. Cracks disappear or decrease in size in the same order. The technique used in this study was sufficient to evaluate the overall deformation of the AAM specimens that occurs in the early stages of curing. Further study could determine the individual cause of this deformation, such as chemical shrinkage/expansion or autogenous (ASTM Standard C 1698-09) and drying shrinkage (ASTM Standard C 1608-07).

## Acknowledgments

Development of AAM is part of the ERA-MIN FLOW project, which has received funding from the Ministry of Education, Science and Sport (acronym: MIZS) under grant agreement No. C 3330-18-252010

## References

- Chen, T.A, Chen, J.H., Huang, J.S. Effects of activator and ageing process on the compressive strengths of alkali-activated glass inorganic binders. *Cem. Concr. Res.* 2017, 76, 1-12.
- Češnovar, M., Traven, K., Horvat, B., Ducman, V. The Potential of Ladle Slag and Electric Arc Furnace Slag use in Synthesizing Alkali Activated Materials; the Influence of Curing on Mechanical Properties *Materials* 2019, 12(7), 1173.
- Fernandez-Jimenez, A., Garcia-Lodeiro, I., Palomo, A. Development of new Cementitious Materials by Alkaline Activating Industrial By-Products. 2nd International Conference on Innovative Materials, Structures and Technologies, Materials Science and engineering 2015, 96, 012005.
- Fernandez-Jimenez, A., de la Torre, A.G., Palomo, A. Lopez-Olmo, G., Alonso, M.M., Aranda, M.A.G. Quantitative determination of phases in the alkali activation of fly ash. Part I. Potential ash reactivity. *Fuel* 2006, 85, 625-634.

- Gudmundsson, J.G., Long-Term Creep and Shrinkage in Concrete Using Porous Aggregate – The Effect of Elastic Modulus. Master Thesis, University of Reykjavik, Iceland, 2013.
- Jensen, O.M., Hansen, P.F. Autogenous deformation and RH-change in perspective. *Cem. Concr. Res.* 2001, 31, 1859-1865.
- Lura, P., Jensen, O.M., Van Breugel, K. Autogenous shrinkage in high- performance cement paste: An evaluation of basic mechanisms, *Cem. Concr. Res.* 2003, 33, 223-232.
- Li, Z., Zhang, S., Zuo, Y., Ye, G. Chemical deformation of metakaolin based geopolymer, *Cem. Concr. Res.* 2019, 120, 108-118.
- Li, Z., Liu, J., Ye, G. Drying shrinkage of alkali-activated slag and fly ash concrete. A comparative study with ordinary Portland cement concrete. In proceedings of the Workshop on Concrete Modelling and Materials Behaviour in honour of Professor Klaas van Breugel, Delft, The Netherlands, 27-29 August 2018, p.p. 160-166.
- Mastali, M., Kinnunen, P., Dalvand, A., Mohammadi Firouz, R., Ilikainen, M. Drying shrinkage in alkali-activated binders – A critical review. *Con. Build. Mat.* 2018, 190, 533-550.
- Mobili, A., Belli, A., Giosue, C., Bellezze, T., Tittarelli, F. Metakaolin and fly ash alkali-activated mortars compared with cementitious mortars at the same strength class, *Cem. Concr. Res.* 2016, 88, 198-210.
- Natali Murri, A., Rickard, W.D.A., Bignozzi, M.C., van Riessen, A. High temperature behaviour of ambient cured alkali-activated materials based on ladle slag. *Cem. Concr. Res.* 2013, 43, 51-61.
- Nedeljković, M., Li, Z., Ye, G. Setting, strength, and Autogenous Shrinkage of alkali-Activated Fly Ash and Slag Pastes: Effect of Slag Content, *Materials*, 2018, 11, 2121.
- van Deventer, J.S.J., Provis, J.L., Duxson, P. Technical and commercial progress in the adoption of geopolymer cement. *Min Eng* 2012; 29:89-104.
- van Jaarsveld, J.g.s., van Deventer, J.S.J. Lukey, G.C. The effect of composition and temperature on the properties of fly ash-and kaolinite-based geopolymers. *Chem. Eng. Jou* 2002, 89, 63-73.